Biochimica et Biophysica Acta, 548 (1979) 616—635

BBA 47763

QUENCHING OF FLUORESCENCE BY TRIPLET EXCITED STATES IN CHLOROPLASTS

JACQUES BRETON [a], NICHOLAS E. GEACINTOV [b] and CHARLES E. SWENBERG [b]

[a] *Service de Biophysique, Departement de Biologie, Centre d' Etudes Nucleaires de Saclay, 91190 Gif-sur-Yvette (France) and* [b] *Chemistry Department, New York University, New York, NY 10003 (U.S.A)*

(Received February 12th, 1979)
(Revised manuscript received June 5th, 1979)

Key words: Fluorescence quenching; Carotenoid; Triplet state; Chloroplast; Chlorophyll

Summary

The fluorescence quantum yield in spinach chloroplasts at room temperature has been studied utilizing a 0.5—4.0 μs duration dye laser flash of varying intensities as an excitation source. The yield (Φ) and carotenoid triplet concentration were monitored both during and following the laser flash. The triplet concentration was monitored by transient absorption spectroscopy at 515 nm, while the yield Φ following the laser was probed with a low intensity xenon flash. The fluorescence is quenched by factors of up to 10—12, depending on the intensity of the flash and the time interval following the onset of the flash. This quenching is attributed to a quencher Q whose concentration is denoted by Q. The relative instantaneous concentration of Q was calculated from Φ utilizing the Stern-Volmer equation, and its buildup and decay kinetics were compared to those of carotenoid triplets. At high flash intensities ($>10^{16}$ photon $\cdot$ cm^{-2}) the decay kinetics of Q are slower than those of the carotenoid triplets, while at lower flash intensities they are similar. Q is sensitive to oxygen and it is proposed that Q, at the higher intensities, is a trapped chlorophyll triplet. This hypothesis accounts well for the continuing rise of the carotenoid triplet concentration for 1—2 μs after the cessation of the laser pulse by a slow detrapping mechanism, and the subsequent capture of the triplet energy by carotenoid molecules.

At the maximum laser intensities, the carotenoid triplet concentration is about one per 100 chlorophyll molecules. The maximum chlorophyll ion concentration generated by the laser pulses was estimated to be below 0.8 ions/

Abbreviation: Chl, chlorophyll

100 chlorophyll molecules. None of the observations described here were altered when a picosecond pulse laser train was substituted for the microsecond pulse.

A simple kinetic model describing the generation of singlets and triplets (by intersystem crossing), and their subsequent interaction leading to fluorescence quenching, accounts well for the observations. The two coupled differential equations describing the time dependent evolution of singlet and triplet excited states are solved numerically. Using a singlet-triplet bimolecular rate constant of $\gamma_{st} = 10^{-8}\ cm^3 \cdot s^{-1}$, the following observations can be accounted for: (1) the rapid initial drop in Φ and its subsequent levelling off with increasing time during the laser pulse, (2) the buildup of the triplets during the pulse, and (3) the integrated yield of triplets per pulse as a function of the energy of the flash.

Introduction

High intensity lasers are now frequently utilized to study dynamical processes in photosynthetic materials. It is thus important to understand the nature of the photophysical processes which can occur at high levels of excitation. In many pulse experiments a large number of photons are absorbed within short time intervals and thus nonlinear intensity-dependent processes can occur. When the density of excitations is high (more than one excitation per photosynthetic unit in a given time interval corresponding to the fluorescence lifetime), annihilation of singlet excitons with a concomitant decrease in the fluorescence yield can occur. Measurements of relative fluorescence quantum yields as a function of the duration in time and the intensity of the laser excitation thus provide information about these non-linear quenching processes.

When picosecond laser pulse trains are used (in which the spacing between adjacent picosecond pulses is ~5 ns) to excite the fluorescence of spinach chloroplasts, quenching states are produced which are relatively long-lived and survive from one picosecond pulse to the next within the pulse train [1]. The accumulation of these quenchers as a function of time gives rise to a decreased fluorescence quantum yield within the succeeding pulses [1,2]. We proposed that these quenchers are either triplet excited states or ions produced by the intense picosecond laser pulses [1,3]. Delosme [4], Zankel [5], Den Haan [6], and Mauzerall [7] have previously proposed that long-lived triplet states act as quenchers of the fluorescence when microsecond duration conventional light flash excitation is employed.

In this work we have utilized a microsecond duration dye laser flash to study the buildup and decay of the long-lived fluorescence quenchers both during and just following the laser flash. The kinetics of these quenchers and the buildup and decay of carotenoid triplets is compared. At relatively low pulse intensities ($\sim 3 \cdot 10^{14}$ photons $\cdot\ cm^{-2}$) the concentration of these quenchers Q appears to be proportional to the concentration of carotenoid triplets. However, when the intensity of the flashes is increased by a factor of 100, Q displays a kinetic behavior different from that of the carotenoid triplets. It is proposed in this work that, particularly at high intensities, Q is a trapped chlorophyll triplet which quenches excited singlet chlorophyll states more strongly than carotenoid triplets.

Experimental Section

Spinach chloroplasts

The details of the preparation of the chloroplasts from whole spinach leaves is described elsewhere [8]. The chloroplasts were suspended in a sucrose (0.4 M)-Tris (20 mM, pH 8.2)-KCl (20 mM) buffer solution. Several drops of this suspension in 75% glycerol (in order to reduce the light scattering) were squeezed between two microscope slide cover slips so that the effective sample thickness was between 0.05 and 0.2 mm.

In order to monitor the laser flash-induced absorbance changes (to monitor the concentration of carotenoid triplets), the chloroplast concentration was adjusted to give an absorbance of 0.4—0.8 at the wavelength of observation (515 nm).

In some experiments it was desirable to observe the effects of gaseous N_2 or O_2 on the kinetics of the fluorescence quenchers and/or carotenoid triplet lifetimes. In these cases the aqueous chloroplast suspension was deposited on a glass slide as usual and was allowed to evaporate to dryness. Oxygen or nitrogen gas was blown directly over the sample.

Measurements of absorbance changes and fluorescence yield changes following the laser pulse

These measurements were performed by using an optical multichannel analyzer (1205A console and 1205D detector head, Princeton Applied Research, Princeton, NJ). The plane of the sample was oriented at a 45° angle with respect to the incident actinic laser beam. A xenon flash, the sample, and the vidicon detector head were oriented along an axis which itself was oriented at a 90° angle to the laser beam (Fig. 1). By a proper selection of filters, either fluorescence quantum yields were measured by firing the xenon flash after a preselected time interval following the laser, or absorbance changes produced during or after the laser pulse were monitored utilizing the same xenon flash. Time resolution was obtained by gating the vidicon detector head utilizing a high voltage pulser (Princeton Applied Research, Model 1211).

The xenon flash pulse width was about 2 μs (full width, half maximum); the discharge of this flash was imaged through a blue filter (Schott BG18) on the sample as a slit about 10 mm in height and 1 mm in width. After traversing the sample, this beam was recollimated on the photosensitive elements of the detector head as a spot of the same size as the 1 × 10 mm image on the sample. The intensity profile of this 10 mm long image of the xenon flash was displayed with a 500 channel resolution on the vidicon-detector console system. The optical multichannel analyzer was used in the gated mode using the 1211 pulse generator. In the transient absorption experiments a 50 ns gating time was used which was timed to coincide with the intensity maximum of the xenon flash. A multichannel digital delay generator was used to synchronize the triggering of the xenon flash and the gating of the detector with respect to the triggering of the actinic laser flash. The initial triggering of this delay generator was provided by a photodiode on which part of the laser flash was incident (Fig. 1). The laser flash was focused on the sample as a small horizontal spot (2 mm wide and 1 mm high) using a slit aperture. The center of

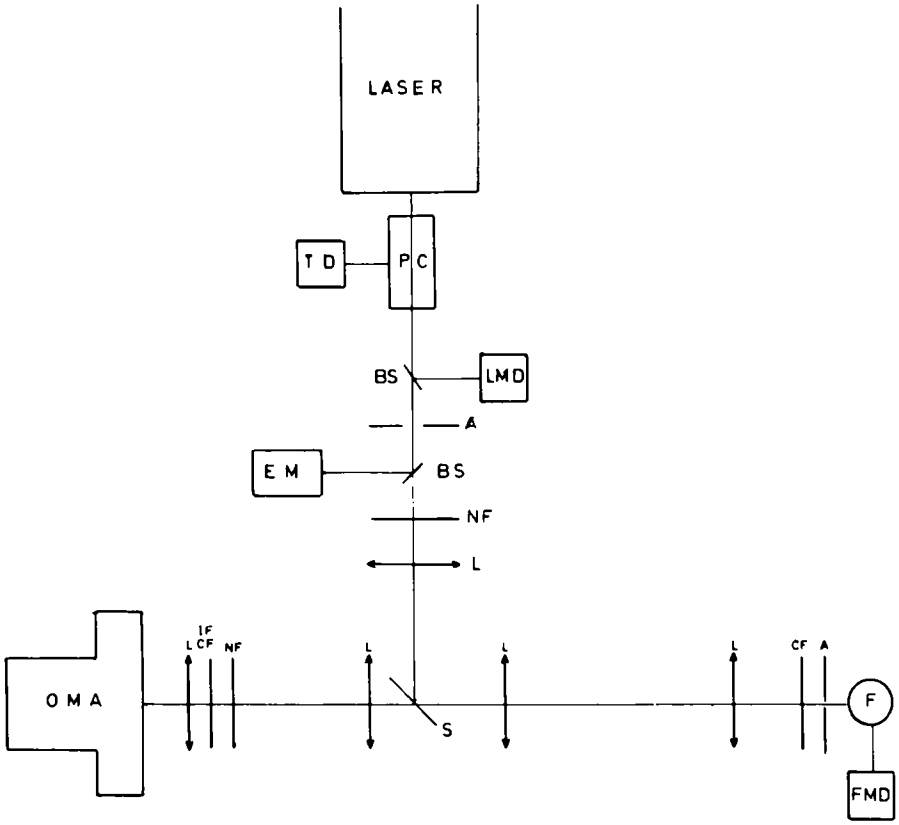

Fig. 1. Schematic diagram of the experimental installation. PC, Pockels cell; TD, trigger diode; LMD, laser intensity monitoring diode; BS, beam splitter; A, aperture; EM, laser energy meter; NF, neutral density filter; L, lenses; F, xenon flash lamp; CF, color filter; S, sample; IF, interference filter; OMA, gated optical multichannel analyzer.

this laser beam and that of the xenon flash were made to coincide on the sample.

For the measurement of absorbance changes at fixed time intervals either within or after the laser flash, an interference filter (3 nm full width half maximum) was positioned in front of the detector head. 3—5 signals were accumulated with the laser flash on ('light' signal) and stored in one of the two memory banks of the 1205A console. An equal number of signals were accumulated in the other memory bank of the console with the actinic laser flash off ('dark' signal). Examples of such light and dark signals are shown in Fig. 2A. The effect of the actinic laser beam was obtained by integration over 20—40 channels corresponding to the maximum of the laser light spot which was conveniently obtained by displaying the contents of the two memory banks in the light minus dark mode (Fig. 2A, curve c). Appropriate analysis and calculations provided the percentage change in the transmitted light (xenon flash) produced by the actinic laser beam.

Kinetic information on these laser produced absorbance changes (the xenon flash itself was too weak to produce observable absorbance changes) were

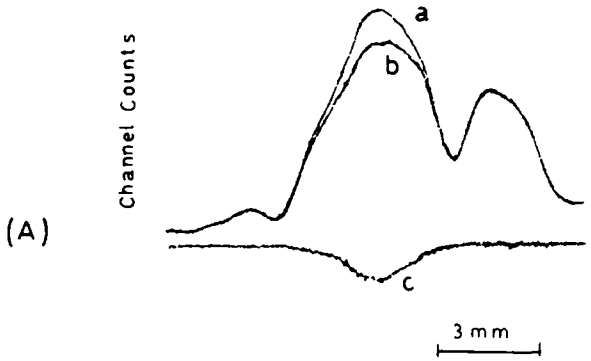

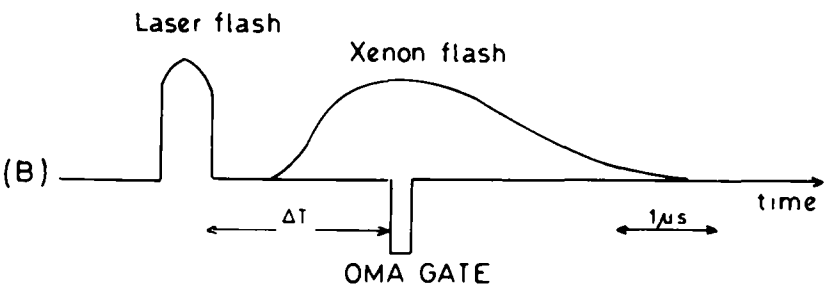

Fig. 2. (A) Intensity distribution of the xenon flash lamp on the OMA detector head after passing through the sample, and after exposing the sample to the actinic laser flash (b) and without the laser flash (a). The difference between these two signals is (c) = (b) — (a). The horizontal scale represents the distance from one end of the illuminated sample to the other (see the text). (B) Relationship, in time, between the actinic laser flash (a 500 ns portion isolated from the 3.7 μs total duration pulse using a Pockels cell is shown), the pulse xenon flash, and the optical multichannel analyzer detector gate. The position of the gate was adjustable by setting the delay time ΔT on the 1211 Pulser. The xenon flash was utilized either to monitor the transient absorption due to carotenoid triplets at 515 nm, or to probe the fluorescence quantum yield after the flash.

obtained by changing the delay between the actinic laser flash and the triggering of the gating pulse and of the xenon flash (Fig. 2B).

The same configuration was utilized to monitor the fluorescence quantum yield increase as a function of time after the termination of the laser pulse. This was achieved by replacing the interference filter used in the absorbance measurements in front of the OMA by a red cut-off filter (Schott RG 665) which allowed the fluorescence to pass, but not the blue excitation light of the xenon flash. The gating time of the optical multichannel analyzer was between

100 and 500 ns which was sufficiently long for a reasonable signal/noise ratio in these fluorescence measurements. In monitoring the fluorescence quantum yield changes as a function of time after the actinic laser pulse, the usual induction effect corresponding to a rise in yield after about 30 μs was observed [9]. This effect was suppressed by providing a continuous background illumination from a He-Ne laser, which was normally used in the alignment of the optics.

The laser pulse

The actinic laser pulse was provided by a model 33 (Electro-Photonics, Belfast, U.K.) laser operated with the dye rhodamine 6G (excitation wavelength 600 nm). The duration of the pulse was of the order of 2 μs (full width, half maximum), but was about 3.7 μs long from the onset of the pulse to its termination. A Pockels cell was utilized when necessary to isolate an approximately constant intensity 500 ns portion of this pulse.

The output energy of the laser was measured by using a 45° beam splitter, which reflected a portion of the total energy onto the detector head of an energy meter (model R 3230, Laser Precision Corporation, Yorkville, NY). The laser beam was attenuated by using metallized calibrated neutral density filters.

Results and Discussion

Fluorescence quenching and carotenoid triplet buildup during the pulse

The basic results are presented in Fig. 3. The time profile of the laser pulse (integrated intensity $7 \cdot 10^{16}$ photons $\cdot$ cm^{-2}) and the relative fluorescence quantum yield $\Phi(t)$ are shown in Fig. 3(A) and 3(B) respectively. The quantity $\Phi(t)$ is calculated by dividing the instantaneous fluorescence intensity by the instantaneous laser intensity, both determined during the same 50-ns gate-time interval. $\Phi(t)$ drops sharply during the first 100 ns while the intensity of the excitation pulse is still rising to its maximum. Beyond 100 ns, the fluorescence yield shows comparatively small variations. The evolution of the carotenoid triplet concentration both during the pulse, and for a period of ~400 ns after the pulse is shown in Fig. 3(C). It is noteworthy that the concentration of carotenoid triplets continues to rise even after the cessation of the laser pulse (500 ns). It reaches a constant level at about 700 ns which is maintained for 1.5—2 μs and only then the carotenoid triplet concentration begins to decline (data not shown). This effect is reproducible in different samples at high laser intensities and clearly represents a time lag in the formation of the carotenoid triplets.

Fluorescence recovery and decay of carotenoid triplets after the pulse

The fluorescence quantum yield recovers after the pulse on time scales of microseconds. However, the recovery time is strongly dependent on the intensity of the actinig pulse (Fig. 4(A)). Thus, for relatively weak laser flashes (intensity $\sim 3 \cdot 10^{14}$ photon $\cdot$ cm^{-2}), the fluorescence quantum yield recovers to its previous value within about 30 μs ($t_{1/2} \cong 5$ μs). This recovery time remains unchanged as the intensity of the pulse is lowered below this value. However when the pulse intensity is increased by a factor of 100, the recovery time of

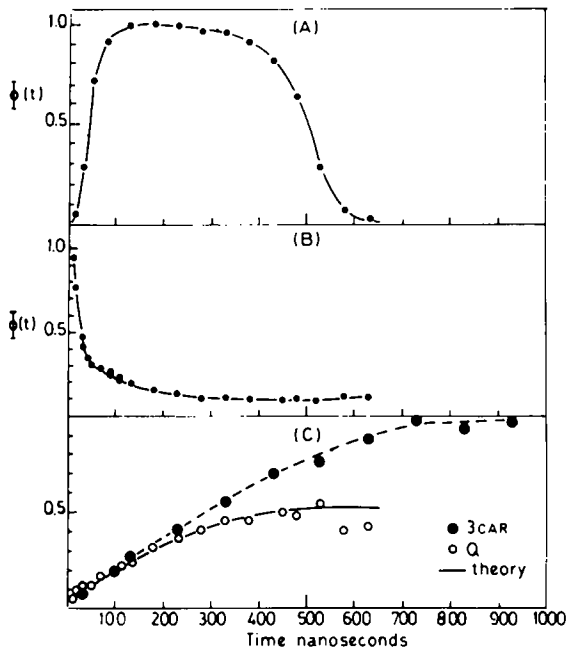

Fig. 3. (A) Intensity distribution as a function of time of the laser pulse. The intensity of this laser pulse was determined using a 50-ns OMA gate by allowing a small fraction of the excitation at 600 nm to reach the OMA detector head. A 500-ns Pockels cell was utilized here to isolate a portion of the pulse. (B) The fluorescence intensity obtained by integrating over the group of optical multichannel analyzer channels corresponding to a wavelength from about 675 to 695 nm. The instantaneous fluorescence quantum yield $\Phi(t)$ is obtained by dividing the instantaneous fluorescence intensity by the instantaneous laser intensity obtained from (A) of this figure. (C) Density of carotenoid triplets (●) and the concentration of Q (○), the fluorescence quencher, obtained from the relative fluorescence quantum yield and the Stern-Volmer equation (1). The solid line (——) represents the calculated triplet exciton density using Eqns. 5 and 6. The integrated flash intensity in these experiments is $7 \cdot 10^{16}$ photons · cm^{-2} per pulse. All experiments done under ambient air atmosphere.

$\Phi(t)$ displays two phases: a rapid one lasting about 45 μs, and a much slower one, accounting for a 10% fluorescence yield loss observable >60 μs after the pulse, and which decays in the millisecond time range.

The decay of the carotenoid triplets after the laser pulse is shown on a semi-logarithmic scale in Fig. 4(B). The $t_{1/2}$ decay time is 5.0 μs for chloroplasts in an air atmosphere and does not appear to depend on the intensity of the flash. The carotenoid triplet decay shown in Fig. 4(B) was obtained by utilizing a high flash intensity ($3 \cdot 10^{16}$ photons · cm^{-2}); a ten-fold decrease in the intensity of the flash did not change this decay time, while the fluorescence recovery was significantly altered. The carotenoid triplet half-life of spinach chloroplasts of ~5 μs in air saturated solution compares reasonably well with the values ranging from 3 to 7 μs obtained by others [10—15].

Calculation of the quencher concentration

In this section, the effective concentration (Q) of the fluorescence quencher is calculated from the fluorescence yield utilizing the Stern-Volmer equation. It is demonstrated that Q cannot be identical to the carotenoid triplets under

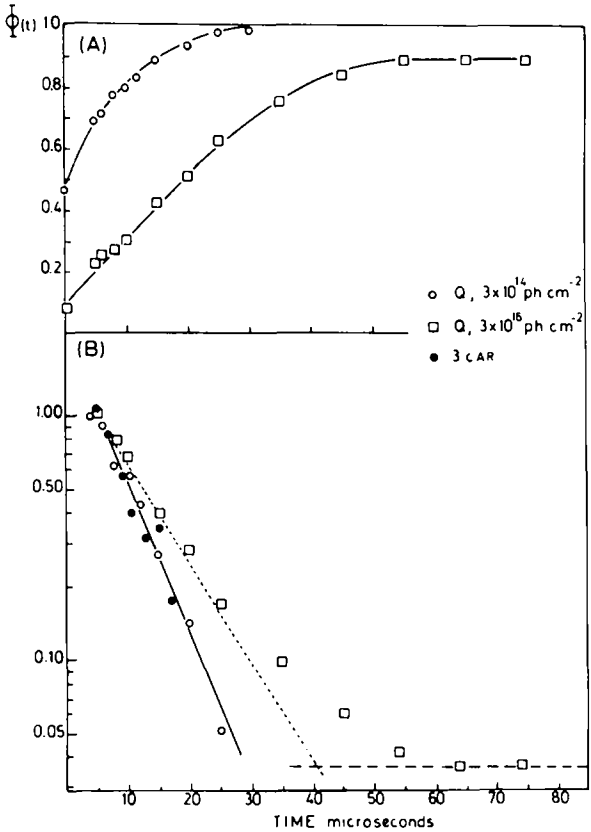

Fig. 4. (A) Relative fluorescence quantum yield of chloroplasts as a function of time after the cessation of a 2-μs (full width, half maximum) actinic laser flash at two different intensities of the laser flash ($3 \cdot 10^{14}$ (○) and $3 \cdot 10^{16}$ (□) photons $\cdot$ cm^{-2} per pulse) (Air atmosphere). (B) semi-logarithmic plot of the decay of carotenoid triplets (•) and Q (□) after the actinic laser flash at the high intensity ($3 \cdot 10^{16}$ photons $\cdot$ cm^{-2} per pulse). Q was calculated from the Stern-Volmer equation (1). ———, exponential decay of carotenoid triplets corresponding to $t_{1/2} = 5.0$ μs. — — —, background concentration of the long-lived fluorescence quencher at $3 \cdot 10^{16}$ photons $\cdot$ cm^{-2} per pulse; the decay of Q can be resolved into two components by subtracting this long-lived component from the data points. - - - - - -, decay of Q after subtracting the long-lived component (— — —) from the actual data points; $t_{1/2}$ of the short-lived Q component is 7.5 μs at the high flash intensity ($3 \cdot 10^{16}$ photons $\cdot$ cm^{-2} per pulse). The decay of Q can be represented by a single exponential decay component with $t_{1/2} = 5.0$ μs at the lower intensity ($3 \cdot 10^{14}$ photons $\cdot$ cm^{-2} per pulse); the decay of Q (○) at this lower intensity is parallel to the decay of carotenoid triplets. It should be noted that the points at $t = 0$ in (A) were obtained by measuring the integrated fluorescence yield during the entire pulse. The measurements of the fluorescence yield and carotenoid triplet concentration were started 4 μs after the onset ($t = 0$) of the laser flash (whose total duration in 3.7 μs) utilizing the probe xenon flash. Thus the points at 4 μs represent the first values obtained after the cessation of the laser flash.

all conditions of excitation. The Stern-Volmer equation is:

$$\frac{F_0}{F} = 1 + K \times Q \qquad (1)$$

where F and F_0 are the fluorescence intensities in the presence and absence, respectively, of the quencher Q. The constant K incorporates the lifetime of the excited state being quenched, the bimolecular encounter rate and the

probability of quenching per encounter. We will use Eqn. 1 in an operational sense to calculate the relative concentration of the quencher present in the chloroplasts both during and after the excitation laser pulse; a more detailed discussion concerning the validity of Eqn. 1 is presented later. Thus, in Fig. 3(C) the relative values of Q calculated from the data in Fig. 3(B) are compared to the experimentally determined carotenoid triplet concentration. Both Q and the carotenoid triplet concentration increase in a parallel fashion with increasing time until about 250 ns, after which the carotenoid triplets continue to rise while Q levels off with increasing time.

Using Eqn. 1, the concentration of Q after the flash is calculated from the data shown in Fig. 4(A), and is plotted as a function of time in Fig. 4(B). At the lower flash intensity the recovery of the fluorescence yield appears to be well correlated with the disappearance of the carotenoid triplets. This is not the case at the higher laser flash intensity; about 20 μs after the flash, the carotenoid triplet concentration is decreased by a factor of ten (corresponding to the limits of the detection of our apparatus), while the fluorescence has recovered to only 50% of its full value.

The quencher Q is a triplet state

The concentration of Q calculated from the relative fluorescence yield shows a different behavior than the concentration of carotenoid triplets towards the end of the laser pulse. The fact that the concentration of Q does not drop off rapidly as the intensity of the laser pulse decreases, clearly demonstrates that Q is not a singlet excited state. As discussed elsewhere [3], the photons arrive at a sufficiently slow rate so that the probability of two short-lived singlet excitons encountering one another is negligible during their lifetime of less than 0.8 ns [16,17]. Under these conditions (microsecond pulse excitation), quenching is due to longer-lived quenchers which we have previously proposed [3] are either excited triplet states, or ions generated by photons absorbed during the earlier intervals within the excitation pulse.

In order to determine if chlorophyll ions play a role in the quenching of the fluorescence, we attempted to monitor laser flash induced absorbance changes at 820 nm, a wavelength at which chlorophyll ions are known to absorb [18]. No absorbance change at 820 nm was observed within the experimental error of ±1%. Assuming therefore that the changes in the transmitted light at 820 nm did not exceed 1%, and from a knowledge of the molar absorption coefficient of chlorophyll ions at 820 nm ($\epsilon(820) = 7000$ lit $\cdot$ M^{-1} $\cdot$ cm^{-1} [19] the maximum number of such chlorophyll ions (Chl^+) per chlorophyll molecule (Chl) in the photosynthetic unit was estimated using the relationship $(Chl^+)/Chl) = [A_{820}/A_{680}][\epsilon(680)/\epsilon(820)]$. The molar extinction coefficient for chlorophyll in vivo at 680 nm is $\epsilon(680) = 3.4 \cdot 10^4$ lit $\cdot$ M^{-1} $\cdot$ cm^{-1}, while A_{680} is the actual absorbance of the samples at 680 nm. Corresponding to a maximum absorbance change of 1%, $A_{820} \leqslant 5 \cdot 10^{-3}$, and utilizing typical experimental data in which A_{680} was about 3.0, we find that even at the highest microsecond pulse laser intensities utilized, $(Chl^+)/(Chl) \leqslant 0.008$, corresponding to less than 2 ions per photosynthetic unit.

Using a picosecond pulse laser train of microsecond duration, the same negative results were obtained. Because of the high peak intensities, multi-

photon absorption effects are possible which, in principle, can give rise to ion pair formation [3]. However, if chlorophyll ions are produced in our picosecond pulse train experiments, their concentrations were too low to be detected.

In order to determine if triplet states were involved in the quenching described earlier, we have investigated the effect of oxygen on the decay time of Q. The influence of paramagnetic gases such as O_2 and NO on carotenoid triplets in spinach chloroplasts has been studied by Mathis and Galmiche [10]. In our experiments we have also observed that the decay of carotenoid triplets is accelerated in an oxygen atmosphere and is lengthened in a nitrogen atmosphere, in a manner similar to that reported by Mathis and Galmiche. A qualitatively similar effect is observed also on the fluorescence recovery time after the pulse both at low and high intensities of excitation. Thus, for example at an intensity of $\sim 10^{16}$ photons $\cdot$ cm^2 per flash, the rapid phase portion of the fluorescence recovery time (cf. Fig. 4(A)) increased from 34 μs in air, to 40 μs in a N_2 atmosphere, while it decreased to 17 μs in an oxygen atmosphere. We thus conclude that Q is an excited triplet state. According to the data in Fig. 4(B), at relatively low laser flash intensities, Q may be identical to the carotenoid triplet because the decay kinetics are the same. However, at the higher flash intensities ($\sim 10^{16}$ photons $\cdot$ cm^{-2} per flash), Q does not appear to be identical to the carotenoid triplets since the decay kinetics are different.

The decay of the longer component ($t > 60$ μs) observed at high flash intensities is insensitive to oxygen and it is therefore not a triplet state. Its nature has not been established in this work, and this component, which corresponds to a ~10% reduction in the fluorescence yield, will not be discussed further.

Comparisons between the kinetic properties of Q and carotenoid triplets

In this section we discuss the relationship between the kinetic behavior of the fluorescence quencher Q and the time dependence of the concentration of carotenoid triplets.

If carotenoid triplets were the sole quenchers of the fluorescence, then the relationship between the experimentally measured F_0/F values and the carotenoid triplet concentration should obey Eqn. 1. A straight line with an intercept of unity should be obtained when F_0/F is plotted as a function of the carotenoid triplet concentration. Such a plot is shown in Fig. 5(A); the data in this figure is taken from the experiment shown in Fig. 3. The values of F_0/F and carotenoid triplets obtained within the same time interval during the laser pulse are plotted against each other. During the initial portion of the 500 ns laser pulse, the points lie along a straight line. However, towards the end of the pulse, when a significant concentration of carotenoid triplets has built up, a significant deviation from this linearity occurs. This deviation is beyond the experimental error and indicates that a quencher other than a carotenoid triplet is active.

The same type of plot is shown in Fig. 5(B) for data obtained after the laser pulse. At the lower excitation flash intensity the Stern-Volmer law appears to be valid, while at the higher intensity it is not.

The linearity at the low flash intensity in Fig. 5(B) also implies that under these conditions Q could be identical to a carotenoid triplet. However, this fact is also consistent with the assumption that the concentration of Q is simply

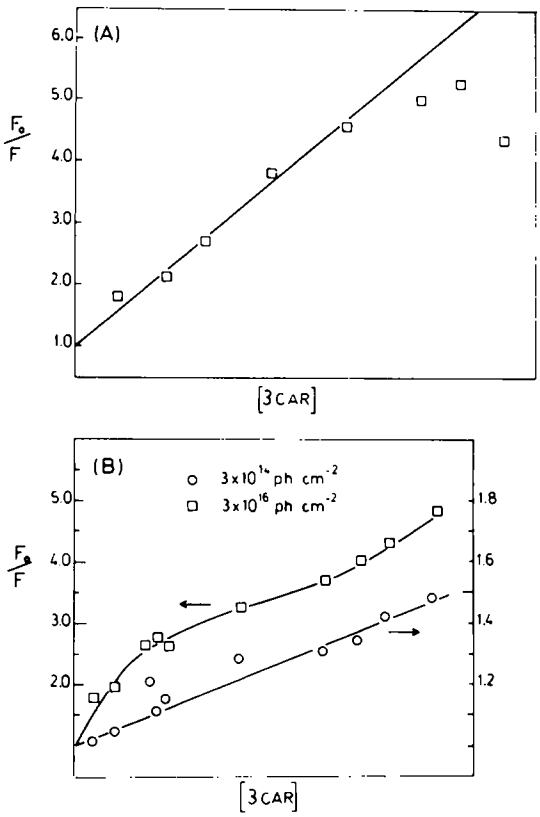

Fig. 5. (A) Stern-Volmer (Eqn. 1) plot of F_0/F, the relative fluorescence yield, as a function of the carotenoid triplet concentration. The data are taken from Fig. 3(A) and Fig. 3(B); the data points refer to the fluorescence yields and carotenoid triplet concentration during the laser flash. (B) Stern-Volmer plots of relative fluorescence yields and carotenoid triplet concentration after the actinic laser flash of two different intensities (o, $3 \cdot 10^{14}$; □, $3 \cdot 10^{16}$ photons · cm^{-2} per pulse).

proportional to the concentration of carotenoid triplets. From our results alone it is thus not possible to state whether carotenoid triplets are, or are not the sole quenchers of the chlorophyll *a* fluorescence at the lower flash intensities.

Relative quenching efficiencies — carotenoid and chlorophyll triplets

It has been proposed [11,20] that in chloroplasts the chlorophyll triplet lifetime is limited by rapid (~40 ns) energy transfer to carotenoids according to the following scheme:

$$^3\text{Chl} + \text{Car} \rightarrow {}^3\text{Car} + \text{Chl} \qquad (2)$$

where Car and Chl represent a carotenoid and a chlorophyll molecule in their ground states respectively. The superscript '3' denotes triplet states. Thus, since the lifetime of the carotenoid triplets should be about 100 times longer, the steady state concentration of chlorophyll triplets should be about two orders of magnitude lower than that of the carotenoid triplets.

There are both theoretical reasons and experimental evidence supporting

the idea that the efficiency of quenching of excited chlorophyll singlets (Chl *) by carotenoid triplets should be lower than the quenching of Chl * by chlorophyll triplets.

We compare the two following quenching processes:

$$\text{Chl} * + {}^3\text{Chl} \rightarrow \text{Chl} + {}^3\text{Chl} * \quad (3)$$

$$\text{Chl} * + {}^3\text{Car} \rightarrow \text{Chl} + {}^3\text{Car} * \quad (4)$$

The asterisks indicate higher excited states. According to standard theories of energy transfer [21], the efficiencies of quenching of the chlorophyll singlets depend on the overlap between the emission spectrum of the donor (Chl *) and the absorption spectrum of the acceptor (^{3}Chl or ^{3}Car). For Chl * the emission spectrum lies above 680 nm, while the triplet-triplet absorption spectrum for $^3\text{Car} \rightarrow {}^3\text{Car} *$ lies below 600 nm [13,14]. However, there is a finite absorbance for the process $^3\text{Chl} \rightarrow {}^3\text{Chl} *$ above 680 nm [22], thus providing reasonable donor-acceptor overlap for the quenching of chlorophyll singlets by chlorophyll triplet states (Eqn. 3). We therefore conclude that quenching of chlorophyll singlets by carotenoid triplets should be less effective than quenching by chlorophyll triplets in photosynthetic systems containing chlorophyll and carotenoids.

Utilizing various mutants of *Rhodopseudomonas sphaeroides* chromatophores and ruby laser excitation, Monger and Parson [23] showed that the carotenoid triplets were about 4—5 times less effective than bacteriochlorophyll triplets as quenchers of the bacteriochlorophyll fluorescence. Furthermore, in these mutants, plots of F_0/F against the concentration of either the carotenoid or the bacteriochlorophyll triplet concentration gave straight lines, showing that the Stern-Volmer equation is obeyed. This result is different from the one obtained in chloroplasts (Fig. 4).

Trapped chlorophyll triplets

Mathis [15] observed that the risetime of the carotenoid triplets following a nanosecond laser excitation is less than 200 ns. This result is consistent with the rapid decay of chlorophyll triplets according to Eqn. 2 in chloroplasts [20]. Thus, about 200 ns following their generation by the laser pulse, there are no mobile or free chlorophyll triplet excitons which are capable of transferring their energy to carotenoids according to these experiments [15,20]. In our experiments, however, the duration of the laser pulse is significantly longer than the transfer time from ^{3}Chl to ^{3}Car and trapped chlorophyll triplets which are not able to transfer their energy to carotenoids may be created; the energy transfer processes (Eqn. 3) require nearest-neighbor contact exchange interaction to be effective on the time scales of microseconds. Thus, if there are no carotenoid molecules in the immediate vicinity of a trapped chlorophyll triplet, its lifetime should be longer than 200 ns. Such trapped chlorophyll triplets, even at a low concentration, may still contribute more effectively to the fluorescence quenching than the more abundant carotenoid triplets, according to the considerations outlined in the previous section. The slow rise and levelling off in the carotenoid triplet concentration for 1—1.5 μs after the cessation of the laser pulse indicates that there exists a source of triplet excited states,

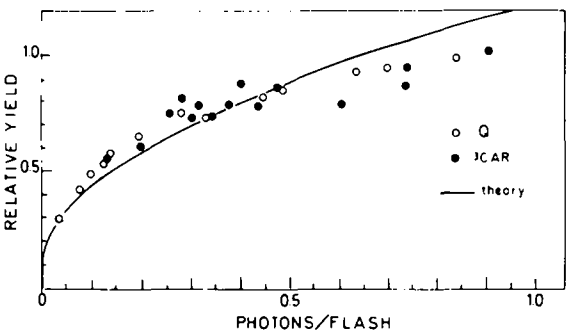

Fig. 6. Plot of relative total yield of quenchers, Q, and carotenoid triplets, ^{3}Car, as a function of integrated flash intensity. Maximum absorbed integrated intensity (1.0 on horizontal scale) $G(t) = 4.2 \cdot 10^{19}$ photons $\cdot$ cm^{-3} (incident intensity of $3 \cdot 10^{16}$ photons $\cdot$ cm^{-2} per pulse). Solid line is the theoretical triplet exciton density, n_t, at the termination of pulse obtained by numerical integration of Eqns. 5 and 6: $K = 1.4 \cdot 10^8$ s^{-1}, $\gamma_{ss} = 5.2 \cdot 10^{-9}$ cm$^3 \cdot$ s^{-1}, $\gamma_{st} = 7.0 \cdot 10^{-9}$ cm$^3 \cdot$ s^{-1}, $\beta_t = 1.6 \cdot 10^5$ s^{-1}, $\beta_s = 1.25 \cdot 10^9$ s^{-1}, the experimental and theoretical data were normalized with respect to each other at the point corresponding to 0.5 relative photons per flash.

which is capable of generating additional amounts of carotenoid triplets, even when no further photons are being absorbed. We therefore propose that at high laser intensities trapped chlorophyll triplets are created or become apparent, which compete with carotenoid triplets in the quenching of chlorophyll singlets. This hypothesis can account for the slow continuing rise of carotenoid triplets after the excitation has ceased by assuming a slow partial detrapping of chlorophyll triplets and their subsequent capture by carotenoid molecules. It must be cautioned however that we have no direct evidence that a chlorophyll triplet is involved in this process. We know only that the fluorescence quencher is a triplet state (effect of oxygen) and that it is not a carotenoid triplet, since in that case it would exhibit an absorption band at 515 nm characteristic of carotenoid triplets in various biological and nonbiological environments [11,12].

Concentration of triplet states

The dependence of the relative concentrations of Q (calculated from experimental values of F_0/F measured 5 μs after the flash and utilizing Eqn. 1), and the carotenoid triplet concentration on the energy of the laser flash are shown in Fig. 6. Within experimental error, the ratio ^{3}Car/Q appears to be constant. The concentration displays a characteristic fast rise with increasing energy at low flash intensities, and a slower increase as the flash energy is increased still further. The utilization of a picosecond pulse train instead of a microsecond pulse gives the same results as in Fig. 6. Thus, a similar number of carotenoid triplets are produced in both the microsecond and the picosecond pulse train cases.

Mathis [14] has also observed the type of curve shown in Fig. 6 in his studies of the concentration of carotenoid triplets in chloroplasts as a function of the energy of a ruby laser flash. Furthermore, similar results were also obtained by Monger et al. [23,24] in bacterial chromatophores; these latter workers qualitatively attributed the shapes of these curves to singlet-triplet

exciton quenching which decreases the lifetime of the singlets. This reduction in the singlet exciton lifetime not only gives rise to a decrease in the fluorescence yield, but also to a decrease in the yield of triplets as the flash intensity is increased [23]. In the next section we formulate a quantitative scheme and demonstrate that the type of data shown in Fig. 6 can be indeed accounted for in terms of this singlet-triplet exciton quenching model.

It is of interest to determine the concentration of carotenoid triplets produced at the maximum flash intensity to provide an absolute vertical scale in Fig. 6. This can be done by utilizing the method described earlier for the determination of the relative chlorophyll ion concentration. Typical transmittance changes at 515 nm were ~20% at the maximum laser intensities. With the molar absorption coefficient for carotenoid triplets being 10^5 lit $\cdot$ M^{-1} $\cdot$ cm^{-1} [25], we obtain about one carotenoid triplet per 100 chlorophyll molecules. For each reaction center in spinach chloroplasts there are a total of 230 chlorophyll and 48 carotenoid molecules [26] per photosynthetic unit. Based on these values, the maximum number of carotenoid triplets per photosynthetic unit is 2. Thus, relatively few of the carotenoid molecules in a given unit are in the triplet excited state. Any free chlorophyll triplet excitons present even at the highest flash energies should be able to transfer their energy to the remaining carotenoid molecules in a photosynthetic unit. The appearance of chlorophyll triplets in the high laser intensity limit thus cannot be due to a depletion of ground state carotenoid molecules. A sufficient number of carotenoid molecules are present at all times to accept the energy from chlorophyll triplets.

Kinetic model of fluorescence quenching by singlet-triplet exciton fusion

In this section a simple kinetic model including the generation of triplets by intersystem crossing from singlets, the quenching of singlet excitons by triplets and singlets is described. The two coupled differential equations describing the time dependence of singlet excitons, $n_s(t)$, and of triplet excitons, $n_t(t)$, are solved numerically. In this exciton-exciton annihilation model we have neglected for simplicity any of the structural and molecular heterogeneity of the photosynthetic unit. It has been shown previously [27,28] that fluorescence quantum yield curves as a function of single picosecond laser flash intensity can also be interpreted in terms of such a model when singlet-singlet annihilation is considered only. In this work, however, the duration of the laser pulse is $\geqslant$500 ns, and thus there is sufficient time for the triplet density to build up, necessitating the inclusion of singlet-triplet annihilation processes. The relative contributions of singlet-singlet and singlet-triplet exciton annihilation as a function of the laser pulse duration are also estimated.

The kinetic model is one in which the incident laser pulse, whose intensity profile is described by $G(t)$ photons $\cdot$ cm^{-3} $\cdot$ s^{-1}, generates chlorophyll singlets whose concentration is $n_s(t)$ $\cdot$ cm^{-3}. These singlet excitons decay by unimolecular rate processes with a rate constant $\beta_s(s^{-1})$, which include fluorescence and intersystem crossing to create triplet excitons. Exciton-exciton annihilation is denoted by the appropriate bimolecular rate constants γ_{ss} and γ_{st} (singlet-singlet and singlet-triplet annihilation, respectively).

The coupled differential equations governing the concentration of singlet

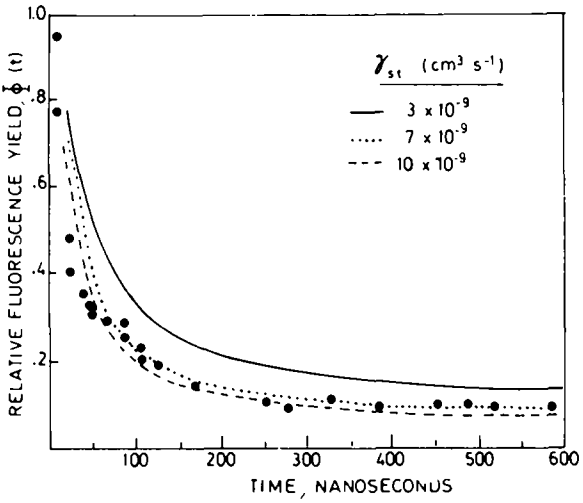

Fig. 7. The instantaneous relative fluorescence yield $\Phi(t)$ as a function of time. Eqns. 5 and 6 were solved numerically with the experimental pulse shape given in Fig. 3(A) with total absorbed integrated pulse intensity, $G(t) = 9.8 \cdot 10^{19}$ photon $\cdot$ cm^{-3} (incident intensity $7 \cdot 10^{16}$ photons $\cdot$ cm^{-2} per pulse). Experimental points, •. Parameters: $\beta_s = 1.25 \cdot 10^9$ s^{-1}; $\beta_t = 1.6 \cdot 10^5$ s^{-1}; $K = 1.4 \cdot 10^8$ s^{-1} and $\gamma_{ss} = 5.2 \cdot 10^{-9}$ cm$^3 \cdot$ s^{-1}; (———) $\gamma_{st} = 3 \cdot 10^{-9}$ cm$^3 \cdot$ s^{-1}; (- - - - -) $\gamma_{st} = 7 \cdot 10^{-9}$ cm$^3 \cdot$ s^{-1}, and (— —) $\gamma_{st} = 10 \cdot 10^{-9}$ cm$^3 \cdot$ s^{-1}.

and triplet excitons are:

$$\frac{dn_s}{dt} = G(t) - \beta_s n_s - \tfrac{1}{2}\gamma_{ss} n_s^2 - \gamma_{st} n_s n_t \tag{5}$$

$$\frac{dn_t}{dt} = K n_s - \beta_t n_t \tag{6}$$

where $K(s^{-1})$ is the rate of triplet generation and $\beta_t(s^{-1})$ is the triplet decay rate. The number of photons absorbed, $G(t) \cdot cm^{-3} \cdot s^{-1}$, is related to the incident intensity $I(t)$ (photons $\cdot$ cm$^{-2} \cdot$ s^{-1}) by the relationship $G(t) = \alpha I(t)$, where $\alpha = 1.4 \cdot 10^3$ cm^{-1} (600 nm) is obtained by utilizing the relationship $\alpha(cm^{-1}) = c(M \cdot lit^{-1}) \times \epsilon(lit \cdot M^{-1} \cdot cm^{-1})$. The molar extinction coefficient is derived from the data of Schwartz [29], while c is the concentration of chlorophyll in vivo ($c = 0.1$ M), which is derived from the data of Park and Biggins [30]. The total number of photons absorbed per cm^3 per pulse is then $F_t = \int_0^\infty G(t)dt$.

In Eqns. 5 and 6 we do not specify whether the triplet exciton density n_t refers to carotenoid, or free and/or trapped chlorophyll triplets. Separate specification of all the dynamical processes involving these different triplet species would necessitate solving four coupled non-linear equations. It can be shown that these four equations can be reduced to Eqns. 5 and 6 with n_t identified as the concentration of mobile chlorophyll triplet excited states under the following conditions: (1) The trapped chlorophyll triplet density is proportional to the concentration of carotenoid triplets, and (2) the mobile chlorophyll triplet excitons maintain steady state. The first assumption results from the fact that the trapped chlorophyll triplet, assumed to be Q at high

laser intensities, has a similar lifetime to that of the carotenoid triplets. The validity of the steady state assumption for free chlorophyll triplets is a consequence of their fast trapping rate [20]. In this more complex model the parameters K and γ_{st} in Eqns. 5 and 6 are no longer interpreted as the singlet-triplet intersystem crossing rate and the bimolecular singlet-triplet exciton annihilation rate constant respectively, but are now functions of (1) the annihilation rate constants of singlet excitons by the different types of triplets present, (2) the trapping rates of mobile chlorophyll triplets, and (3) the relative concentrations of the different triplet species. At this point the relative contributions of these different triplets, the relative annihilation rate constants and trapping rates are not sufficiently well known to warrant the treatment of these four coupled equations, since this would involve too many unknown parameters. In the simplified Eqns. 5 and 6 therefore, the quantities γ_{st}, K and β_t are thus to be regarded as effective rate constants, and n_t as the effective concentration of triplets.

The coupled differential Eqns. 5 and 6 were solved on a CDC 6600 computer using standard numerical methods to solve ordinary differential equations [31]. The experimentally determined shape of the laser pulse (Fig. 3A) was digitized into 16.6-ns intervals and an integration mesh size of 15 picoseconds was selected. The computer output for a given incident intensity consisted of the instantaneous singlet ($n_s(t)$) and triplet ($n_t(t)$) exciton densities as a function of time. The instantaneous fluorescence quantum yield, $\Phi(t)$, was calculated according to

$$\Phi(t) = K_r \frac{n_s(t)}{G(t)} \tag{7}$$

where K_r is the radiative rate constant; however, $\Phi(t)$ is always expressed in relative units and thus the exact value of K_r is unimportant. The time dependence of $\Phi(t)$ within the laser pulse was calculated using the following values of the various rate parameters: $K = 1.4 \cdot 10^8\ s^{-1}$ [27], $\beta_s = 1.25 \cdot 10^9\ s^{-1}$ [11,12], $\gamma_{ss} = 5.2 \cdot 10^{-9}\ cm^3 \cdot s^{-1}$ [24] and $\beta_t = 1.6 \cdot 10^5\ s^{-1}$; this value of β_t is the reciprocal of the triplet lifetime, which is taken to be $\sim 5\ \mu s$; the calculations are insensitive to the exact value of β_t, as long as β_t is longer than the duration of the laser pulse; this assumption is also consistent with the data which shows that both Q and the carotenoid triplets, the two possible long-lived quenchers in our experiments, exhibit decay times in the microsecond range. The singlet-triplet annihilation rate constant was treated as an adjustable parameter. The results of these calculations utilizing three different value of β_{st} are shown in Fig. 7. The fit to the experimental data is satisfactory considering the crudity of the model. Of importance here is that a simple singlet-triplet exciton quenching model can reproduce the essential features of the experiment, (1) the rapid decrease of $\Phi(t)$ within the first 50—100 ns of the laser pulse, and (2) the subsequent levelling off in the quantum yield. The values of the adjustable parameter γ_{st} which give the best fits to the data ($\gamma_{st} \approx 10^{-8}\ cm^3 \cdot s^{-1}$) are in excellent accord with the theoretical predictions of the chlorophyll singlet-chlorophyll triplet quenching rate constant calculated by Rahman and Knox [21]. However, this agreement could also be fortuitous because γ_{st} is an effective quenching rate constant as discussed above.

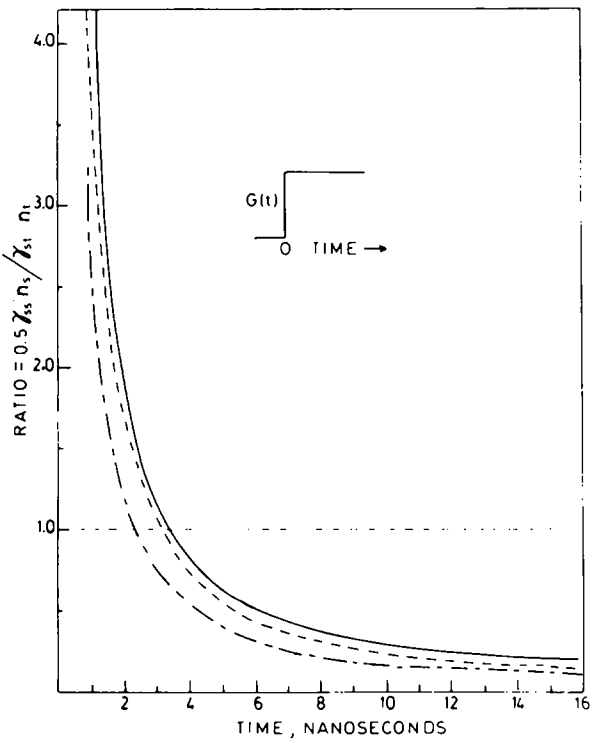

Fig. 8. The instantaneous relative importance of the singlet-singlet and singlet-triplet bimolecular terms in Eqn. 5, for an excitation square wave pulse $G(t)$ (see insert). Parameters used in solving Eqns. 5 and 6 are: $\beta_s = 1.25 \cdot 10^{-9}$ s^{-1}; $\beta_t = 1.6 \cdot 10^{5}$ s^{-1}; $K = 1.4 \cdot 10^{8}$ s^{-1}; $\gamma_{ss} = 5.2 \cdot 10^{-9}$ cm$^3 \cdot$ s^{-1}; $\gamma_{st} = 7 \cdot 10^{-9}$ cm$^3 \cdot$ s^{-1}. Excitation source intensities (———) $G(t) = 10^{24}$ photons $\cdot$ cm$^{-3} \cdot$ s^{-1}; (- - - - -) $G(t) = 10^{26}$ photons $\cdot$ cm$^{-3} \cdot$ s^{-1}; (— - — -) $G(t) = 10^{28}$ photons $\cdot$ cm$^{-3} \cdot$ s^{-1}.

Calculation of the time dependence of the triplet concentration within the laser pulse

The validity of these calculations can be further checked by calculating the time dependence of the triplet concentration n_t within the pulse and comparing these values with those of Q, where the latter is deduced from the experimental $\Phi(t)$ curve (Fig. 3B) utilizing the Stern-Volmer equation.

The use of the Stern-Volmer equation (our Eqn. 1) is normally justified under steady state conditions. Justification of our use of Eqn. 1 in deducing the quencher concentration Q from the experiment in view of Eqns. 5 and 6 follows, since both the singlet and triplet exciton density risetimes are rapid, and for $t > 10$ ns are relatively constant during the pulse. These remarks are justified in Fig. 9 which illustrates that the relative integrated quantum yield is approximately constant for times greater than 10 ns.

The comparison between the calculated quantities n_t from Eqns. 5 and 6, and Q calculated from the data and Eqn. 1, is shown in Fig. 3(C). In calculating the n_t curve, a value of $\gamma_{st} = 10^{-8}$ cm$^3 \cdot$ s^{-1} was chosen which gives the best fit to the $\Phi(t)$ curve (Fig. 7). The vertical scale for the theoretical n_t curve was adjusted to give the best superimposition on the experimental points. It is

evident from Fig. 3(C) that good agreement is obtained between the n_t curve and Q, but not with the measured carotenoid triplet concentration within the pulse. This result is consistent with the hypothesis that quenching by carotenoid triplets is less important than quenching by Q, which we have tentatively identified as a trapped chlorophyll triplet.

The flash energy dependence of the calculated triplet concentration

The experimental dependence of Q and ^{3}Car on the flash intensity are shown in Fig. 6. The numerical integration method, if correct, should reproduce not only the instantaneous values of $\Phi(t)$ and Q, but also the total number of triplets n_t produced by a pulse of given intensity. This comparison between the normalized triplet exciton density (denoted by the solid line) as computed according to Eqns. 5 and 6, and the experimentally determined quencher density Q, is shown in Fig. 6. The experimental and theoretical data were normalized with respect to each other at the relative photons per flash values of 0.50, which corresponds to an incident intensity of $1.5 \cdot 10^{16}$ photons $\cdot$ cm^{-2} per pulse. A good fit is obtained except near the maximum values of the flash energy, where the theory predicts a slightly higher triplet quencher concentration than is observed experimentally. At the higher triplet exciton densities, triplet-triplet annihilation may become sufficiently important to reduce the triplet density somewhat. This effect was previously proposed by Mathis [14] and may account for the difference between the experimental and the calculated values of triplets at high flash energies, since a triplet-triplet annihilation term was not included in Eqn. 6.

Relative importance of singlet-singlet and singlet-triplet annihilations

In previous calculations of fluorescence quantum yields as a function of the laser flash intensities, it was assumed that singlet-triplet annihilations can be neglected when the duration of the laser pulses is of the order of 7 ns or less [28]. Intuitively, such an approximation appeared to be justified because it requires a finite time interval for a triplet population of any significance to build up when singlet-singlet annihilations are neglected. To examine the validity of this approximation we have numerically integrated the coupled nonlinear differential Eqns. 5 and 6 for a step like excitation pulse; i.e.: $G(t)$ equals a constant for $t>0$ (see insert in Fig. 8). In Fig. 8 the instantaneous ratio (R) of the nonlinear singlet-singlet ($\frac{1}{2}\gamma_{ss}n_s^2$) and singlet-triplet ($\gamma_{st}n_t n_s$) annihilation terms are shown for three different flash intensities. The dominance of the singlet-singlet annihilation term ($R \gg 1$) for short pulses is clearly evident thereby justifying the neglect of singlet-triplet interactions for single picosecond pulse studies [27]. Also evident is the dominance of singlet-triplet quenching for longer pulses. The relative total quantum yield defined as

$$\Phi_T(t) = \int_0^\infty \Phi(t)\mathrm{d}t \tag{8}$$

was also calculated for a square wave excitation pulse of different duration from 0 to 25 ns. This was done in order to demonstrate the effect of including only singlet-singlet, or both singlet-singlet and singlet-triplet exciton annihila-

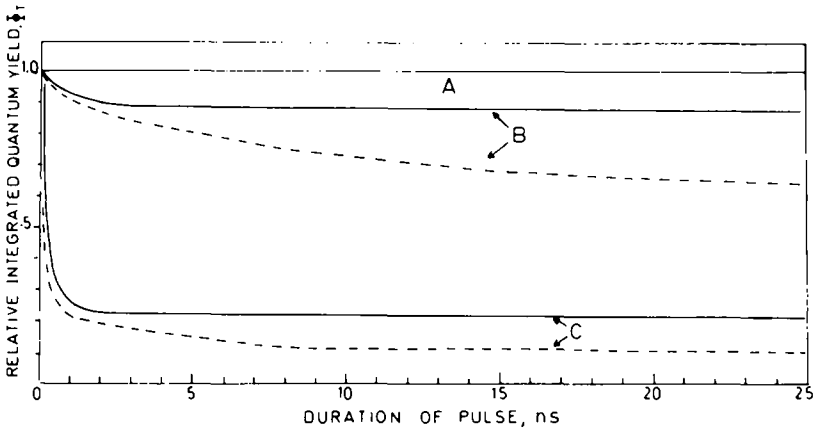

Fig. 9. Relative integrated quantum yield of fluorescence Φ_T as a function of square wave pulse duration calculated by numerically integrating Eqns. 5 and 6 of text with $K = 1.4 \cdot 10^8\ s^{-1}$; $\beta_t = 1.6 \cdot 10^5\ s^{-1}$; $\beta_s = 1.25 \cdot 10^9\ s^{-1}$. Curves (A) $\gamma_{ss} = 0$; $\gamma_{st} = 0$; (B) $G(t) = 10^{26}$ photons $\cdot$ cm$^{-3} \cdot s^{-1}$; (C) $G(t) = 10^{28}$ photons $\cdot$ cm$^{-3} \cdot s^{-1}$. For both (B) and (C): Solid line (———) $\gamma_{ss} = 5.2 \cdot 10^{-9}$ cm$^3 \cdot s^{-1}$, $\gamma_{st} = 0$. Dashed line (- - - - -) $\gamma_{ss} = 5.2 \cdot 10^{-9}$ cm$^3 \cdot s^{-1}$, $\gamma_{st} = 7 \cdot 10^{-9}$ cm$^3 \cdot s^{-1}$.

tion terms in the theoretical analysis of fluorescence quantum yield vs. pulse intensity curves [28]. The same set of parameters β_t, β_s, γ_{ss}, γ_{st}, and K, as before, were utilized; it should be noted that a change by a factor of two in the less well-known parameters β_t and K does not alter the conclusions. Lowering either β_t or K shifts the curves in the same manner as a lower incident photon intensity.

The results for two different incident intensities ($G(t) = 10^{26}$ (curve B) and $G(t) = 10^{28}$ (curve C) photons $\cdot$ cm$^{-3} \cdot s^{-1}$) are shown in Fig. 9. In curve A, $\gamma_{ss} = \gamma_{st} = 0$, while in curves B and C the effects of γ_{ss} only (solid line), and of γ_{ss} and γ_{st} (dashed lines), are shown on Φ_T as a function of the pulse length. The two flux values of 10^{26} and 10^{28} photons $\cdot$ cm$^{-3} \cdot s^{-1}$ correspond approximately to 0.5 and 50 hits per nanosecond respectively per photosynthetic unit, assuming a unit size of ~300 chlorophyll molecules. It is evident that even for a 7 ns pulse, the effects of triplets cannot be ignored; at the lower intensity for a pulse of 7 ns, the calculated yield for $\gamma_{st} = 0$ is 0.87, while it is 0.76 when the singlet-triplet interactions are included. At the higher intensity the effect of triplets is more pronounced, the analogous drop is from 0.21 to 0.12 for a pulse of 7 ns. Thus, singlet-triplet interactions can be neglected only when the pulse duration is in the picosecond range.

In summary, while the kinetic model utilized here is crude and ignores the exact nature of the triplet states which act as fluorescence quenchers, it accounts semiquantitatively for the following experimental observations: (1) the rapid initial drop and subsequent levelling off in the fluorescence quantum yield (Fig. 3(B)), (2) the time dependence of the quencher concentration Q (Fig. 3(C)), and (3) the laser flash intensity dependence of the triplet concentration (Fig. 6).

Acknowledgements

The authors acknowledge stimulating discussions with P. Mathis, G. Paillotin and E. Roux. The portion of this work performed at New York University (N.E. Geacintov and C.E. Swenberg) was supported by National Science Foundation Grant PCM 76-14359.

References

1 Breton, J. and Geacintov, N.E. (1976) FEBS Lett. 69, 86—89
2 Porter, G., Synowiec and Tredwell, C.T. (1977) Biochim. Biophys. Acta 459, 329—336
3 Geacintov, N.E. and Breton, J. (1977) Biophys. J. 17, 1—15
4 Delosme, R. (1972) in Proceedings of the 2nd International Congress on Photosynthesis Research (Forti, G., Avron, M. and Melandri, A., eds.), pp. 187—195, Junk, The Hague
5 Zankel, K.L. (1973) Biochim. Biophys. Acta 325, 138—148
6 Den Haan, G.A., Duysens, L.N.M. and Egberts, D.J.N. (1974) Biochim. Biophys. Acta 368, 409—421
7 Mauzerall, D. (1976) J. Phys. Chem. 80, 2306—2309
8 Breton, J., Roux, E. and Whitmarsh, J. (1975) Biochem. Biophys. Res. Commun. 64, 1274—1277
9 Mauzerall, D. (1972) Proc. Natl. Acad. Sci. U.S.A. 69, 1358—1362
10 Mathis, P. and Galmiche, J.M. (1967) C.R. Acad. Sci. 264, 1903—1906
11 Mathis, P. (1970) Thesis, University of Paris, Orsay
12 Mathis, P., Butler, W.L. and Satoh, K. (1979) Photochem. Photobiol., in the press
13 Buchwald, H.E. and Wolff, C.H. (1971) Z. Naturforsch. 26b, 51—53
14 Mathis, P. (1969) in Progress in Photosynthesis Research, Vol. 2 (Metzner, H., ed.), pp. 818—822, Tubingen
15 Mathis, P. (1966) C.R. Acad. Sci. 263, 1770—1772
16 Hervo, G., Paillotin, G. and Thiery, J. (1975) J. Chim. Phys. 72, 761—766
17 Sauer, K. and Brewington, G.T. (1977) in Proceedings of the fourth International Congress on Photosynthesis (Hall, D.O., Coombs, J. and Goodwin, T.W., eds.) pp. 409—421, Biochem. Soc., London
18 Borg, D.C., Fajer, J., Felton, R.H. and Dolphin, D. (1970) Proc. Natl. Acad. Sci. U.S.A. 67, 813—820
19 Seki, H., Arai, S., Shida, T. and Imamura, M. (1973) J. Am. Chem. Soc. 95, 3404—3405
20 Breton, J. and Mathis, P. (1970) C.R. Acad. Sci. 271, 1094—1096
21 Rahman, T.S. and Knox, R.S. (1973) Phys. Stat. Solidi (b) 58, 715—720
22 Linschitz, H. and Sarkanen, K. (1958) J. Am. Chem. Soc. 80, 4826—4832
23 Monger, T.G. and Parson, W.W. (1977) Biochim. Biophys. Acta 460, 393—407
24 Monger, T.G., Cogdell, R.J. and Parson, W.W. (1976) Biochim. Biophys. Acta 449, 136—153
25 Mathis, P. (1969) Photochem. Photobiol. 9, 55—63
26 Lichtenthaler, H.K. and Park, R.B. (1963) Nature 198, 1070—1072
27 Geacintov, N.E., Breton, J., Swenberg, C.E. and Paillotin, G. (1977) Photochem. Photobiol. 26, 629—638
28 Swenberg, C.E., Geacintov, N.E. and Pope, M. (1976) Biophys. J. 16, 1447—1452
29 Schwartz, M. (1972) Methods Enzymol. 24, 139—146
30 Park, R.B. and Biggins, J. (1964) Science 144, 1009—1010
31 Hindmarsh, A.C., Gear: Ordinary differential equation system solver, UCID-30001 Rev. 3, Lawrence Livermore Laboratory, Berkeley, CA